Mon. Not. R. Astron. Soc. **000**, 1–11 (2009) Printed 26 August 2011 (MN LATEX style file v2.2)

Helicity and dynamo action in magnetized stellar radiation zones

G. Rüdiger[1⋆], L. L. Kitchatinov[1,2,3], D. Elstner[1]
[1] *Leibniz-Institut für Astrophysik Potsdam, An der Sternwarte 16, 14482 Potsdam, Germany*
[2] *Institute for Solar-Terrestrial Physics, PO Box 291, Irkutsk 664033, Russia*
[3] *Pulkovo Astronomical Observatory, St. Petersburg, 196140, Russia*

Accepted . Received ; in original form

ABSTRACT
Helicity and α effect driven by the nonaxisymmetric Tayler instability of toroidal magnetic fields in stellar radiation zones are computed. In the linear approximation a purely toroidal field always excites pairs of modes with identical growth rates but with opposite helicity so that the net helicity vanishes. If the magnetic background field has a helical structure by an extra (weak) poloidal component then one of the modes dominates producing a net kinetic helicity anticorrelated to the current helicity of the background field.
The mean electromotive force is computed with the result that the α effect by the most rapidly growing mode has the same sign as the current helicity of the background field. The α effect is found as too small to drive an α^2 dynamo but the excitation conditions for an $\alpha\Omega$ dynamo can be fulfilled for weak poloidal fields. Moreover, if the dynamo produces its own α effect by the magnetic instability then problems with its sign do not arise. For all cases, however, the α effect shows an extremely strong concentration to the poles so that a possible $\alpha\Omega$ dynamo might only work at the polar regions. Hence, the results of our linear theory lead to a new topological problem for the existence of large-scale dynamos in stellar radiation zones on the basis of the current-driven instability of toroidal fields.

Key words: magnetohydrodynamics (MHD) – instabilities – stars: magnetic fields – stars: interiors.

1 INTRODUCTION

Hydromagnetic dynamos can be understood as magnetic instabilities driven by a special flow pattern in fluid conductors. There are, however, strong restrictions on the characteristics of such flows (see Dudley & James 1989) as well as on the geometry of the resulting magnetic fields (Cowling 1933). The restrictions even exclude any dynamo activity for a number of flows. We mention as an example that differential rotation alone can never maintain a dynamo (Elsasser 1946).

An open question is whether magnetic instabilities are able to excite a sufficiently complicated motion that together with a (given) background flow can generate magnetic fields. Tout & Pringle (1992) suggested that nonuniformly rotating disks can produce a dynamo when magnetorotational (MRI) and magnetic buoyancy instabilities are active. Later on, numerical simulations of Brandenburg et al. (1995) and Hawley, Gammie & Balbus (1996) have shown that MRI alone may be sufficient for the accretion disk dynamo. It remains, however, to check (at least for the case of low magnetic Prandtl number) whether the MRI-dynamo has physical or numerical origin (Fromang & Papaloizou 2007; Fromang et al. 2007).

Another possibility was discussed by Spruit (2002) who suggested that differential rotation and magnetic kink-type instability (Tayler 1973) can jointly drive a dynamo in stellar radiation zones. The dynamo if real would be very important for the angular momentum transport in stars and their secular evolution. It taps energy from differential rotation thus reducing the rotational shear. Radial displacements converting toroidal magnetic field into poloidal field are necessary for the dynamo. The dynamo, therefore, unavoidably mixes chemical species in stellar interiors that may have observable consequences for stellar evolution.

Such a dynamo, however, has not yet been demonstrated to exist. The doubts especially concern the kink-type instability that in contrast to MRI exists also without differential rotation. The Tayler instability develops in expense of magnetic energy. Estimations of dynamo parame-

⋆ E-mail: GRuediger@aip.de

ters are thus necessary to assess the dynamo-effectiveness of this magnetic instability.

The basic role in turbulent dynamos plays the ability of correlated magnetic ($\boldsymbol{b}$) fluctuations and velocity ($\boldsymbol{u}$) fluctuations to produce a mean electromotive force along the background magnetic field $\boldsymbol{B}$ and also along the electric current $\boldsymbol{J}$, i.e.

$$\langle \boldsymbol{u} \times \boldsymbol{b} \rangle = \alpha \boldsymbol{B} - \mu_0 \eta_{\rm T} \boldsymbol{J}. \quad (1)$$

We estimate the α effect by Tayler instability in the present paper. We do also find indications for the appearance of the turbulent diffusivity $\eta_{\rm T}$ in the calculations but we do not follow them here in detail. For purely toroidal fields we did *not* find indication for the existence of the term $\boldsymbol{\Omega} \times \boldsymbol{J}$ which can appear in the expression (1) in form of a rotationally induced anisotropy of the diffusivity tensor.

The fluctuating fields for the most rapidly growing eigenmodes and the azimuthal averaging are applied in the LHS of Eq. (1) to estimate the α effect and its relation to the kinetic and magnetic helicity $\mathcal{H}^{\rm kin}$ and $\mathcal{H}^{\rm curr}$. Our linear stability computations do not allow the evaluation of the α effect amplitude but its latitudinal profile and its ratio to the product of rms values of $\boldsymbol{u}$ and $\boldsymbol{b}$ (i.e. the correlation coefficient) can be found. As the differential rotation is necessary for dynamo, we estimate also the influence of differential rotation on Tayler instability. Next, a dynamo model with the parameters estimated for the magnetic instability is designed to find the global modes of the instability-driven dynamo.

2 INSTABILITY AND HELICITY

The model and the stability analysis of this paper are very close to that of Kitchatinov & Rüdiger (2008) and will be discussed here only briefly.

The basic component of the magnetic field inside a star is normally assumed to be the toroidal one. This toroidal field can be produced by differential rotation from even a small poloidal field. The background toroidal field of our model consists of two latitudinal belts of opposite polarities, i.e.

$$\boldsymbol{B} = r \sin\theta \cos\theta \sqrt{\mu_0 \rho}\, \Omega_{\rm A} \boldsymbol{e}_\phi \quad (2)$$

(see Spruit 1999) with $\Omega_{\rm A}$ as the Alfvén frequency of the toroidal field. Spherical coordinates are used with the axis of rotation as the polar axis and $\boldsymbol{e}_\phi$ as the azimuthal unit vector. The latitudinal profile of (2) peaks in mid-latitudes at $\theta = 45°$ and $\theta = 135°$.

The background flow is simply

$$\boldsymbol{U} = r \sin\theta\ \Omega\ \boldsymbol{e}_\phi \quad (3)$$

with Ω as the equatorial rotation rate.

The $\Omega_{\rm A}$ and Ω are radius-dependent but this dependence is not of basic importance for the stability analysis. The reason is that the stratification of the radiative core is stable with positive

$$N^2 = \frac{g}{C_{\rm p}} \frac{\partial S}{\partial r}, \quad (4)$$

where S is the entropy and $C_{\rm p}$ is the specific heat at constant pressure.

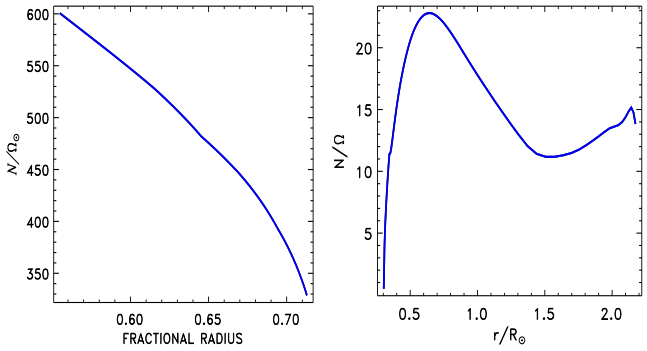

Figure 1. The ratio N/Ω_0 in the radiation zones of the Sun (*left*) and of a 100 Myr old $3M_\odot$ star rotating with 10 days period (*right*). The model of the massive star is computed with the EZ code of Paxton (2004) for $X = 0.7,\ Z = 0.02$.

The buoyancy frequency N is large compared to Ω ($N/\Omega \simeq 400$ in the upper radiative core of the Sun). Then the radial scale of unstable disturbances is short and the dependence of the disturbances on radius can be treated in a local approximation, i.e. in the form of $\exp(\mathrm{i}kr)$. The parameter controlling the stratification influence on the instability is

$$\hat{\lambda} = \frac{N}{\Omega k r}, \quad (5)$$

and the most unstable disturbances have $\hat{\lambda} < 1$ (Kitchatinov & Rüdiger 2008). This means that the radial scale of the disturbances, $\lambda = \pi/k$, is short compared to the radial scale δR of toroidal field or angular velocity variations. In the solar tachocline where Ω strongly varies in radius, the scale ratio is smaller than unity, $\lambda/\delta R \simeq 0.2$ (Kitchatinov & Rüdiger 2009). For such small scale ratio the radial derivatives in the linear stability equations are absorbed by the disturbances so that the local approximation in the radial coordinate can be applied. Note that the unstable modes remain global in horizontal dimensions.

2.1 Instability of toroidal fields

The equation system of the linear stability analysis include

$$\frac{\partial \boldsymbol{u}}{\partial t} + (\boldsymbol{U} \cdot \nabla)\, \boldsymbol{u} + (\boldsymbol{u} \cdot \nabla)\, \boldsymbol{U} + \frac{1}{\mu_0 \rho} \left(\nabla (\boldsymbol{B} \cdot \boldsymbol{b}) - (\boldsymbol{B} \cdot \nabla)\, \boldsymbol{b} - (\boldsymbol{b} \cdot \nabla)\, \boldsymbol{B} \right) = -\left(\frac{1}{\rho} \nabla P \right)' + \nu \Delta \boldsymbol{u} \quad (6)$$

as the momentum equation for the velocity fluctuations and the equations

$$\frac{\partial \boldsymbol{b}}{\partial t} = \nabla \times (\boldsymbol{U} \times \boldsymbol{b} + \boldsymbol{u} \times \boldsymbol{B} - \eta \nabla \times \boldsymbol{b}), \quad (7)$$

for the induction of the magnetic fluctuations and for the disturbances (s) of the entropy

$$\frac{\partial s}{\partial t} + \boldsymbol{U} \cdot \nabla s + \boldsymbol{u} \cdot \nabla S = \frac{C_{\rm p} \chi}{T} \Delta T'. \quad (8)$$

The equations (6)–(8) were reformulated in terms of scalar potentials for toroidal and poloidal parts of the magnetic and velocity fields to reduce the number of equations, i.e.

$$\boldsymbol{u} = -\mathrm{curl}((rW)\boldsymbol{r}) - \mathrm{curl}\ \mathrm{curl}((rV)\boldsymbol{r})$$

$$\boldsymbol{b} = -\mathrm{curl}((rB)\boldsymbol{r}) - \mathrm{curl}\ \mathrm{curl}((rA)\boldsymbol{r}) \tag{9}$$

(Chandrasekhar 1961). The resulting system of five eigenvalue equations can be found elsewhere (Kitchatinov & Rüdiger 2008) and it will here only be extended to the application of helical background fields. Again the eigenvalue problem is solved numerically.

The equations include finite diffusion in opposition to the otherwise similar equations of Cally (2003). The thermal diffusion is especially important because of its destabilizing effect. The Tayler instability requires radial displacements. It does not exist in 2D case of strictly horizontal motion. The radial displacements in radiation zones are opposed by buoyancy. The thermal diffusion smooths out the entropy disturbances to reduce the effect of stable stratification. This largely increases the growth rates for the instability of not too strong, $\Omega_\mathrm{A} < \Omega$, fields (Rüdiger & Kitchatinov 2010). The diffusivities enter the normalized equation via parameters

$$\epsilon_\chi = \frac{\chi N^2}{\Omega_0^3 r^2}, \qquad \epsilon_\eta = \frac{\eta N^2}{\Omega_0^3 r^2}, \qquad \epsilon_\nu = \frac{\nu N^2}{\Omega_0^3 r^2}. \tag{10}$$

In our computations we used the values $\epsilon_\chi = 10^{-4}$, $\epsilon_\eta = 4\times 10^{-8}$, and $\epsilon_\nu = 2\times 10^{-10}$ characteristic for the upper part of the solar radiation zone. As it must be the magnetic Prandtl number ($5\cdot 10^{-3}$) exceeds the ordinary Prandtl number ($2\cdot 10^{-6}$).

The stability problem allows two types of equatorial symmetry of unstable eigenmodes. We use the notations Sm (symmetric mode with azimuthal wave number m) and Am (antisymmetric mode) for these types of symmetry. Sm modes have vector field $\boldsymbol{b}$ which is mirror-symmetric about equatorial plane (symmetric b_r, b_ϕ and antisymmetric b_θ) and mirror-antisymmetric flow $\boldsymbol{u}$ (symmetric u_θ and antisymmetric u_r, u_ϕ). Am modes have antisymmetric $\boldsymbol{b}$ and symmetric $\boldsymbol{u}$. Instability can only be found for nonaxisymmetric disturbances with $m = \pm 1$ in agreement with the stability criteria of Goossens, Biront & Tayler (1981) when applied to the toroidal field model of Eq. (2).

The perturbations are considered as Fourier modes in time, in azimuth and radius in the form $\exp(\mathrm{i}(kr+m\phi-\omega t))$. Only the highest-order terms in kr are used so that in radial direction the theory is a local one (short-wave approximation). The wave number k enters the equations in the normalized form

$$\hat{\lambda} = \frac{N}{\Omega_0 kr} \tag{11}$$

as a ratio of two large numbers. If only toroidal fields are considered with $\Omega_\mathrm{A}/\Omega = 0.1$ Kitchatinov & Rüdiger (2008) found maximal growth rates of order 10^{-4} (normalized with the rotation rate) at radial scales of $\hat{\lambda} \simeq 0.1$ for S1 modes.

As described in KR08, the eigenvalue ω possesses a positive imaginary part for an instability (the growth rate is $\gamma = \Im(\omega)$). The equations have only be solved for the nonaxisymmetric ('kink') modes with $m = \pm 1$. One can easily show that the equation system possesses a symmetry with respect to the change of sign of the azimuthal wave number m. The equations are invariant under the transformation

$$\begin{aligned}&(m, \hat{\omega}, W, V, B, A, S) \rightarrow \\ &\rightarrow (-m, -\hat{\omega}^*, -W^*, V^*, -B^*, A^*, -S^*)\,,\end{aligned} \tag{12}$$

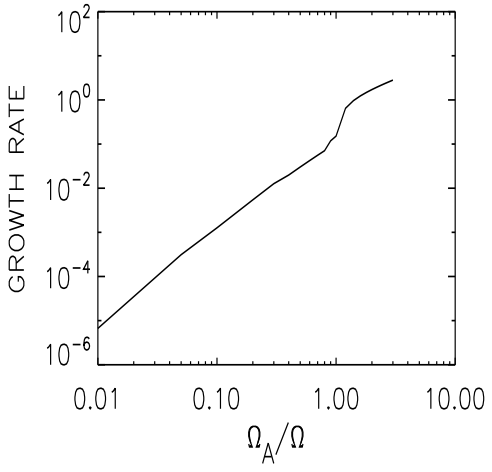

Figure 2. The normalized growth rate $\hat{\gamma} = \Im\omega/\Omega$ of S modes as function of the amplitude of the toroidal background field. Rigid rotation, $m = \pm 1$. Note the slowness of the modes for weak fields with $\Omega_\mathrm{A} < \Omega$ and the jump at $\Omega_\mathrm{A} \simeq \Omega$. The wave numbers are always optimized with respect to the maximum growth rates. $\mathrm{Pm} = 5\cdot 10^{-3}$, $\mathrm{Pr} = 2\cdot 10^{-6}$.

where the asterisks mean the complex conjugate. If an eigenmode exists for $m = 1$ with a certain growth rate γ then the same γ holds for the eigenmode with $m = -1$. We shall demonstrate the importance of this finding for the generation of helicity and α effect.

Figure 2 shows the growth rates for S$\pm$1 modes in dependence of field strength. The results for A$\pm$1 modes are very similar. For weak fields, $0.01 < \Omega_\mathrm{A}/\Omega < 1$ the growth rates are closely reproduced by the parabolic law $\gamma \simeq 0.1\Omega_\mathrm{A}^2/\Omega$. For strong fields, $\Omega_\mathrm{A} > \Omega$, they are proportional to the field strength, $\gamma \simeq \Omega_\mathrm{A}$ and do not depend on the rotation rate.

2.2 Helicity production

All averaging procedures in the present paper are realized by integration over the azimuth coordinate. Consider the formation of the kinetic helicity

$$\mathcal{H}^\mathrm{kin} = \langle \boldsymbol{u} \cdot \mathrm{curl}\ \boldsymbol{u} \rangle, \tag{13}$$

(only the real parts of both factors) whose definition depends on the handedness of the used coordinate system. We shall prefer the righthand system. Let the expressions

$$W = (w_\mathrm{R} + \mathrm{i}w_\mathrm{I})\mathrm{e}^{\mathrm{i}\phi}, \qquad V = (v_\mathrm{R} + \mathrm{i}v_\mathrm{I})\mathrm{e}^{\mathrm{i}\phi}, \tag{14}$$

represent the potential functions W and V. Then the real part of (13) after the integration over the azimuth results to

$$\begin{aligned}\mathcal{H}^\mathrm{kin} = \frac{1}{\sin^2\theta}\Bigg[&\left(mw_\mathrm{I} + \sin\theta\frac{\partial v_\mathrm{I}}{\partial\theta}\right)\left(mv_\mathrm{I} + \sin\theta\frac{\partial w_\mathrm{I}}{\partial\theta}\right) + \\ &+ \left(mw_\mathrm{R} + \sin\theta\frac{\partial v_\mathrm{R}}{\partial\theta}\right)\left(mv_\mathrm{R} + \sin\theta\frac{\partial w_\mathrm{R}}{\partial\theta}\right)\Bigg].\end{aligned} \tag{15}$$

It is easy to show with the transformation rules (12) that this expression for the modes with negative m has the opposite

sign as for the modes with positive m. Hence,

$$\mathcal{H}^{\rm kin}(m=-1) = -\mathcal{H}^{\rm kin}(m=1) \quad (16)$$

(see Fig. 3, bottom). It means that for every unstable mode with finite helicity there is another unstable mode with the same growth and drift rates but with opposite helicity so that the resulting net helicity should vanish. Obviously, if all modes are excited the instability of a purely toroidal axisymmetric field can not produce finite values of the kinetic helicity. The same argument leads to the same conclusion for the current helicity

$$\mathcal{H}^{\rm curr} = \langle \boldsymbol{b} \cdot {\rm curl}\ \boldsymbol{b} \rangle. \quad (17)$$

There is also a more straightforward argument with the same result. The mode $m = -1$ is identical to the mode $m = 1$ but considered in a lefthand coordinate system. The sign of the helicity is equal in both lefthand systems and righthand systems. Hence, the mode $m = -1$ which gives the same helicity in the lefthand system as the mode $m = 1$ in the righthand system yields a negative helicity in the righthand system if the mode $m = 1$ yields a positive helicity in the righthand system. The net helicity in both the righthand system and the lefthand system, therefore, vanishes . Again the same is true for the current helicity (17).

3 INFLUENCE OF POLOIDAL FIELDS

We find (see, however, Cally 2003) that from symmetry reasons unstable purely toroidal fields do not produce a net helicity. An additional poloidal component of the background field, however, breaks the symmetry as then, for example, the two modes possess two different growth rates so that a certain sign of helicity will be preferred (Gellert, Rüdiger & Hollerbach 2011).

In the short-wave approximation only the radial component of the poloidal field is important. We write

$$B_r = r\sqrt{\mu_0 \rho}\ \Omega_{\rm A,p}(\mu) \quad (18)$$

with $\mu = \cos\theta$. Using the notation by KR08 with the operator

$$\hat{\mathcal{L}} = \frac{1}{\sin\theta}\frac{\partial}{\partial\theta}\sin\theta\frac{\partial}{\partial\theta} + \frac{1}{\sin^2\theta}\frac{\partial^2}{\partial\phi^2}, \quad (19)$$

the equation for the azimuthal flow reads

$$\begin{aligned}
&\hat{\omega}\left(\hat{\mathcal{L}}W\right) = -{\rm i}\frac{\epsilon_\nu}{\hat{\lambda}^2}\left(\hat{\mathcal{L}}W\right) + m\hat{\Omega}\left(\hat{\mathcal{L}}W\right) - m\hat{\Omega}_{\rm A}\left(\hat{\mathcal{L}}B\right)\\
&-mW\frac{\partial^2}{\partial\mu^2}\left(\left(1-\mu^2\right)\hat{\Omega}\right) + mB\frac{\partial^2}{\partial\mu^2}\left(\left(1-\mu^2\right)\hat{\Omega}_{\rm A}\right)\\
&+\left(\hat{\mathcal{L}}V\right)\frac{\partial}{\partial\mu}\left(\left(1-\mu^2\right)\hat{\Omega}\right) - \left(\hat{\mathcal{L}}A\right)\frac{\partial}{\partial\mu}\left(\left(1-\mu^2\right)\hat{\Omega}_{\rm A}\right)\\
&+\left(\frac{\partial}{\partial\mu}\left(\left(1-\mu^2\right)^2\frac{\partial\hat{\Omega}}{\partial\mu}\right) - 2\left(1-\mu^2\right)\hat{\Omega}\right)\frac{\partial V}{\partial\mu}\\
&-\left(\frac{\partial}{\partial\mu}\left(\left(1-\mu^2\right)^2\frac{\partial\hat{\Omega}_{\rm A}}{\partial\mu}\right) - 2\left(1-\mu^2\right)\hat{\Omega}_{\rm A}\right)\frac{\partial A}{\partial\mu}\\
&-\frac{1}{\hat{\lambda}}\left(\hat{\Omega}_{\rm A,p}\left(\hat{\mathcal{L}}B\right) + (1-\mu^2)\frac{\partial\hat{\Omega}_{\rm A,p}}{\partial\mu}\frac{\partial B}{\partial\mu} - m\frac{\partial\hat{\Omega}_{\rm A,p}}{\partial\mu}A\right) \quad (20)
\end{aligned}$$

The equation includes the poloidal background field via its last line. The parameter measuring the effect of the poloidal field is

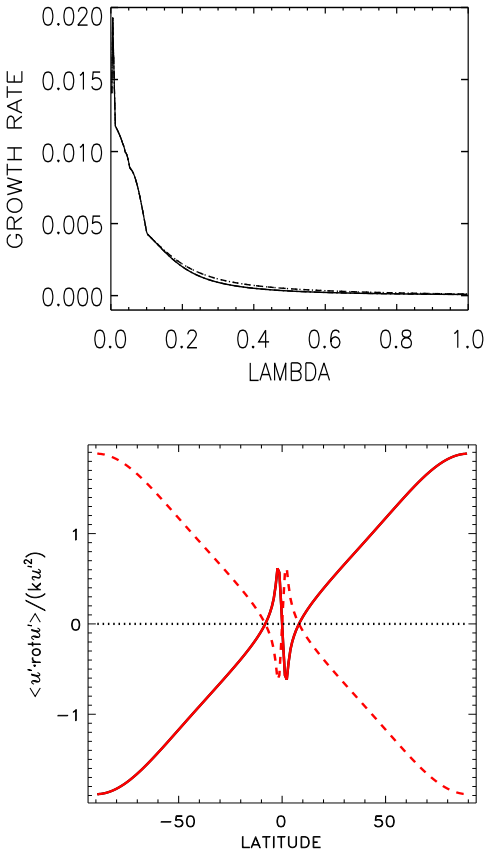

Figure 3. Purely toroidal fields for rigid rotation. Top: The growth rate $\hat{\gamma}$ for $\hat{\Omega}_{\rm A} = 0.3$ vs. the radial scale $\hat{\lambda}$ of the perturbations $A\pm1$ and $S\pm1$. Bottom: The normalized small-scale helicity (13). Solid line: $m = 1$, dashed line $m = -1$. The net helicity vanishes if both modes are simultaneously excited. $B_r = 0$, $\hat{\lambda} = 0.1$.

$$\hat{\Omega}_{\rm A,p} = \frac{N}{\Omega}\frac{\Omega_{\rm A,p}}{\Omega} = \frac{NB_r(\mu)}{\Omega_0^2 r\sqrt{\mu_0\rho}}. \quad (21)$$

Equation (21) shows that the characteristic strength of the field that can influence the Tayler instability ($\hat{\Omega}_{\rm A,p} \sim 1$) is Ω_0/N times the toroidal field amplitude. This factor is of the order $10^{-(2...3)}$.

For the latitudinal profile of the radial field component the simplest choice, i.e. $B_r(\mu) \sim \mu$, is used. Hence, both the background field components B_r and B_ϕ are antisymmetric with respect to the equator. The large-scale current helicity $\boldsymbol{B}\cdot{\rm curl}\boldsymbol{B}$, therefore, is also antisymmetric with respect to the equator. For positive amplitudes $\Omega_{\rm A}$ and $\Omega_{\rm A,p}$ it is *positive* at the northern hemisphere and negative at the southern hemisphere (it runs with $\cos^3\theta$). We shall see that the pseudoscalar $\boldsymbol{B}\cdot{\rm curl}\boldsymbol{B}$ alone determines the behavior of the pseudoscalars $\mathcal{H}^{\rm kin}$ and also of $\mathcal{H}^{\rm curr}$. The basic rotation which via $\boldsymbol{g}\cdot\boldsymbol{\Omega}$ can also form a pseudoscalar does not play here an important role.

The ratio β of the toroidal field amplitude and the radial field amplitude is

$$\beta = \frac{B_\phi}{B_r} = \frac{\hat{\Omega}_{\rm A}}{\hat{\Omega}_{\rm A,p}}\frac{N}{\Omega}. \quad (22)$$

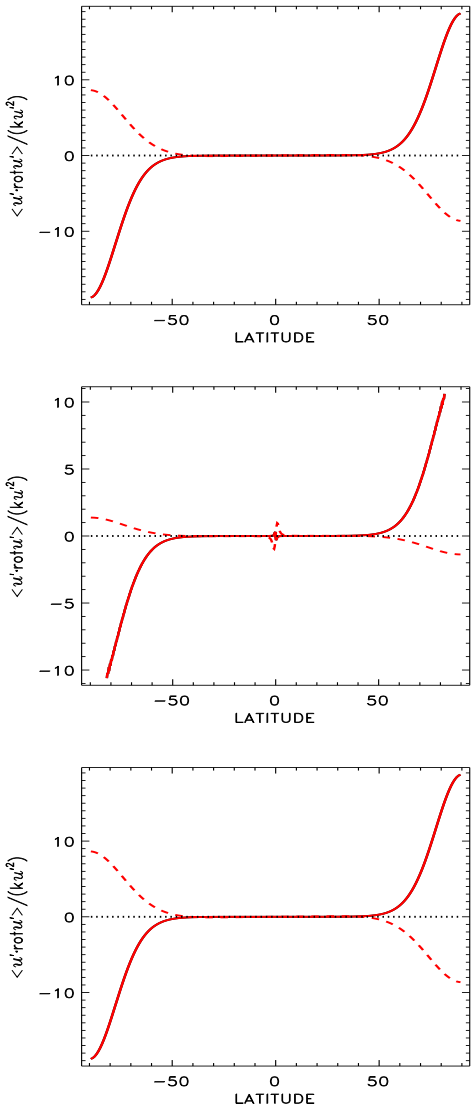

Figure 4. Helical background field. Latitudinal profile of the helicity by the unstable modes S±1 (top) and A±1 (middle) for $\hat{\Omega}_{\rm A} = 0.3$ and $\hat{\Omega}_{\rm A,p} = 0.1$. Solid line: $m = 1$, dashed line: $m = -1$. The net helicity does no longer vanish if both modes are excited. It is $\beta = 3N/\Omega$. Bottom: the S±1 modes for $\Omega = 0$.

The equation for the meridional flow is

$$\hat{\omega}\left(\hat{\mathcal{L}}V\right) = -\hat{\lambda}^2\left(\hat{\mathcal{L}}S\right) - \mathrm{i}\frac{\epsilon_\nu}{\hat{\lambda}^2}\left(\hat{\mathcal{L}}V\right)$$
$$-2\mu\hat{\Omega}\left(\hat{\mathcal{L}}W\right) - 2\left(1-\mu^2\right)\frac{\partial\left(\mu\hat{\Omega}\right)}{\partial\mu}\frac{\partial W}{\partial\mu} - 2m^2\frac{\partial\hat{\Omega}}{\partial\mu}W$$
$$+2\mu\hat{\Omega}_{\rm A}\left(\hat{\mathcal{L}}B\right) + 2\left(1-\mu^2\right)\frac{\partial\left(\mu\hat{\Omega}_{\rm A}\right)}{\partial\mu}\frac{\partial B}{\partial\mu} + 2m^2\frac{\partial\hat{\Omega}_{\rm A}}{\partial\mu}B$$
$$-m\hat{\Omega}_{\rm A}\left(\hat{\mathcal{L}}A\right) - 2m\frac{\partial\left(\mu\hat{\Omega}_{\rm A}\right)}{\partial\mu}A - 2m\left(1-\mu^2\right)\frac{\partial\hat{\Omega}_{\rm A}}{\partial\mu}\frac{\partial A}{\partial\mu}$$
$$+m\hat{\Omega}\left(\hat{\mathcal{L}}V\right) + 2m\frac{\partial\left(\mu\hat{\Omega}\right)}{\partial\mu}V + 2m\left(1-\mu^2\right)\frac{\partial\hat{\Omega}}{\partial\mu}\frac{\partial V}{\partial\mu}$$
$$-\frac{1}{\hat{\lambda}}\left(\hat{\Omega}_{\rm A,p}\left(\hat{\mathcal{L}}A\right)+(1-\mu^2)\frac{\partial\hat{\Omega}_{\rm A,p}}{\partial\mu}\frac{\partial A}{\partial\mu}-m\frac{\partial\hat{\Omega}_{\rm A,p}}{\partial\mu}B\right) \quad (23)$$

The equations for the magnetic fields components are

$$\hat{\omega}\left(\hat{\mathcal{L}}B\right) = -\mathrm{i}\frac{\epsilon_\eta}{\hat{\lambda}^2}\left(\hat{\mathcal{L}}B\right) + m\hat{\mathcal{L}}\left(\hat{\Omega}B\right) - m\hat{\mathcal{L}}\left(\hat{\Omega}_{\rm A}W\right)$$
$$-m^2\frac{\partial\hat{\Omega}}{\partial\mu}A - \frac{\partial}{\partial\mu}\left(\left(1-\mu^2\right)^2\frac{\partial\hat{\Omega}}{\partial\mu}\frac{\partial A}{\partial\mu}\right)$$
$$+m^2\frac{\partial\hat{\Omega}_{\rm A}}{\partial\mu}V + \frac{\partial}{\partial\mu}\left(\left(1-\mu^2\right)^2\frac{\partial\hat{\Omega}_{\rm A}}{\partial\mu}\frac{\partial V}{\partial\mu}\right)$$
$$-\frac{1}{\hat{\lambda}}\left(\hat{\Omega}_{\rm A,p}\left(\hat{\mathcal{L}}W\right)+(1-\mu^2)\frac{\partial\hat{\Omega}_{\rm A,p}}{\partial\mu}\frac{\partial W}{\partial\mu} - m\frac{\partial\hat{\Omega}_{\rm A,p}}{\partial\mu}V\right)$$

and

$$\hat{\omega}\left(\hat{\mathcal{L}}A\right) = -\mathrm{i}\frac{\epsilon_\eta}{\hat{\lambda}^2}\left(\hat{\mathcal{L}}A\right) + m\hat{\Omega}\left(\hat{\mathcal{L}}A\right) - m\hat{\Omega}_{\rm A}\left(\hat{\mathcal{L}}V\right)$$
$$-\frac{1}{\hat{\lambda}}\left(\hat{\Omega}_{\rm A,p}\left(\hat{\mathcal{L}}V\right)+(1-\mu^2)\frac{\partial\hat{\Omega}_{\rm A,p}}{\partial\mu}\frac{\partial V}{\partial\mu}-m\frac{\partial\hat{\Omega}_{\rm A,p}}{\partial\mu}W\right) \quad (24)$$

The entropy equation is not influenced by the poloidal field.

We computed the helicity $\mathcal{H}^{\rm kin}$ of the critical modes always for the amplitude $\hat{\Omega}_{\rm A} = 0.3$ and $\hat{\Omega}_{\rm Ap} = 0.1$ with and without basic rotation. The results are given in Fig. 4.

The solid (dashed) lines give the helicity profiles for $m = 1$ ($m = -1$). Indeed, the helicity of the single modes is antisymmetric with respect to the equator (as also the current helicity of the background field). The plot at the bottom of Fig. 4 for the two modes S1 is for $\Omega = 0$. Note the extremely small differences to the top plot for the same modes under the influence of rotation. It is obviously the pseudoscalar $\boldsymbol{B}\cdot\mathrm{curl}\boldsymbol{B}$ directing the formation of the helicities rather than the pseudoscalar $\boldsymbol{g}\cdot\boldsymbol{\Omega}$ formed by the global rotation.

Figure 5 shows the normalized growth rates $\hat{\gamma} = \gamma/\Omega$ vs the normalized wave length $\hat{\lambda}$ for three different poloidal field amplitudes. From top to bottom: $\hat{\Omega}_{\rm A,p} = 0.3$, $\hat{\Omega}_{\rm A,p} = 0.1$, $\hat{\Omega}_{\rm A,p} = 0.05$. The peaks for the modes with $m = -1$ drift from $\hat{\lambda} = 0.45$ to $\hat{\lambda} = 0.015$. The corresponding peak values of the growth rates dramatically grow from 10^{-6} to 10^{-2} demonstrating the strong stabilization of the Tayler instability for helical fields. An increase of the poloidal field amplitude by a factor of 6 (from bottom to top) leads to a reduction of the growth rate by three orders of magnitude.

The main information of Fig. 5 is that the growth rates of the modes with $m = 1$ and $m = -1$ strongly differ. Obviously, they always produce helicity of opposite signs and with different growth rates. The growth rate for the S1 mode with $m = -1$ exceeds the growth rate of $m = 1$ by a factor of four. It is, however, much smaller than the rotation rate. The unstable Tayler modes are thus very slow, their corresponding growth times are much longer than the rotation periods. The helicity by the $m = -1$ mode is *negative* at the north pole opposite to the current helicity of the background field. The small-scale kinetic helicity and the large-scale current helicity are anticorrelated (cf. Gellert, Rüdiger & Hollerbach 2011, for a similar result in cylinder symmetry).

4 THE ALPHA-EFFECT

Linear stability computations do not provide the absolute value of α. Only its latitudinal profile and its relative mag-

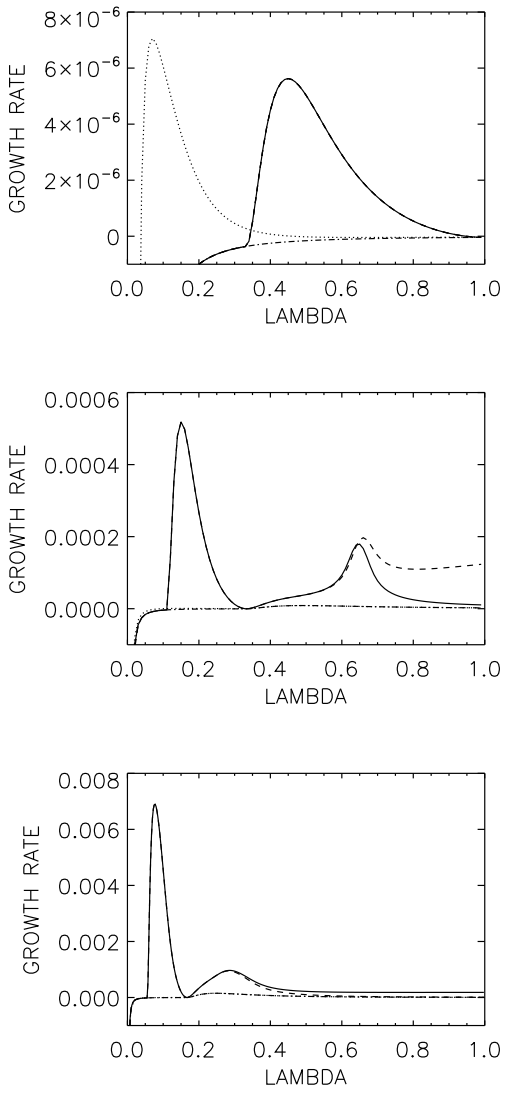

Figure 5. The normalized growth rates $\hat{\gamma}$ for the modes A±1 and S±1 for $\hat{\Omega}_{\rm A} = 0.3$ vs. the normalized wavelength $\hat{\lambda}$. From top to bottom: $\hat{\Omega}_{\rm A,p} = 0.3$, $\hat{\Omega}_{\rm A,p} = 0.1$, $\hat{\Omega}_{\rm A,p} = 0.05$. The modes with $m = -1$ (solid line: S-mode, dashed line: A-mode) possess higher growth rates than the modes with $m = 1$ (dash-dotted: S-mode, dotted A-mode). From top to bottom the growth rates strongly increase while the characteristic length scale decreases. The product $\hat{\gamma}\hat{\lambda}^2$ has always the value of about 10^{-6}.

nitude can be evaluated. We computed the normalized electromotive force

$$\mathcal{E} \;=\; \frac{N}{\Omega}\frac{\langle \boldsymbol{u}\times\boldsymbol{b}\rangle_\phi}{u_{\rm rms}b_{\rm rms}}, \qquad (25)$$

which in opposition to the helicity (Fig. 4) is symmetric with respect to the equator. $u_{\rm rms}$ is the rms velocity fluctuation after horizontal averaging (longitude and latitude), $b_{\rm rms}$ is the rms magnetic fluctuation. The factor N/Ω is introduced because the horizontal (velocity and magnetic) fluctuations are larger than the radial fluctuations by just this factor. With these normalizations the expression (25) is of order unity independent of the actual value of N/Ω.

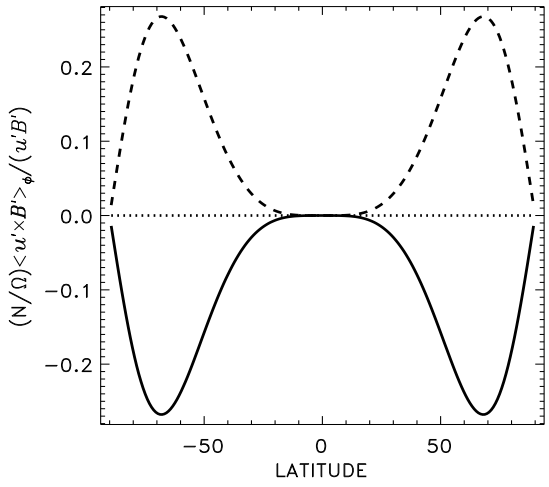

Figure 6. The same as in Fig. 3 (bottom) but for the normalized electromotive force after Eq. (25) for the modes with $m = 1$ (solid) and $m = -1$ (dashed). $\hat{\Omega}_{\rm A,p} = 0$.

Figure 6 gives the main results for purely toroidal fields with (2). The azimuthal component of the electromotive force i) vanishes at the equator, ii) the profile is symmetric with respect to the equator and iii) it is highly concentrated to the poles. The first finding is naturally for the α effect but it is *not* for the term $\boldsymbol{\Omega}\times\boldsymbol{J}$ which could appear in the expression of the turbulence-induced electromotive force as a consequence of a rotationally induced anisotropy of the diffusivity tensor. We find, therefore, this effect not existing due to the Tayler instability of toroidal fields. For more complex field pattern its existence of cannot be excluded but it remained small in any case.

For purely toroidal fields even the α effect does not exist as the modes with opposite sign of m (which have the same growth rates) do cancel each other not only with respect to their helicities but also with respect to the resulting EMF. In the nonlinear regime a spontaneous parity breaking may happen as it has been described by Chatterjee et al. (2010) and by Gellert et al. (2011). In this case, however, it might be impossible to predict the sign and the amplitude of the α effect.

The concentration of helicity and EMF towards the poles reflects a basic property of the Tayler instability, i.e. that the instability pattern is more present in polar regions rather than in equatorial regions (Spruit 1999; Cally 2003).

Figure 5 shows the normalized growth rates $\hat{\gamma}$ as a function of the radial scale $\hat{\lambda}$ under the influence of poloidal field components. The plots shows drastic differences of the growth rates between the modes of $m = 1$ (dotted lines) and $m = -1$ (solid lines). E.g., for $\hat{\Omega}_{\rm A,p} = 0.1$ both modes with $m = -1$ possess the maximum growth rates $\hat{\gamma}$ with $5 \cdot 10^{-4}$ at a wavelength of $\hat{\lambda} = 0.15$. The figure shows a very strong influence of the poloidal field amplitude on the growth rates. The growth rates are small for strong poloidal field but they are large for weak poloidal field. We are thus confronted with the dilemma that only background fields with finite current helicity originate fluctuations with α effect but the

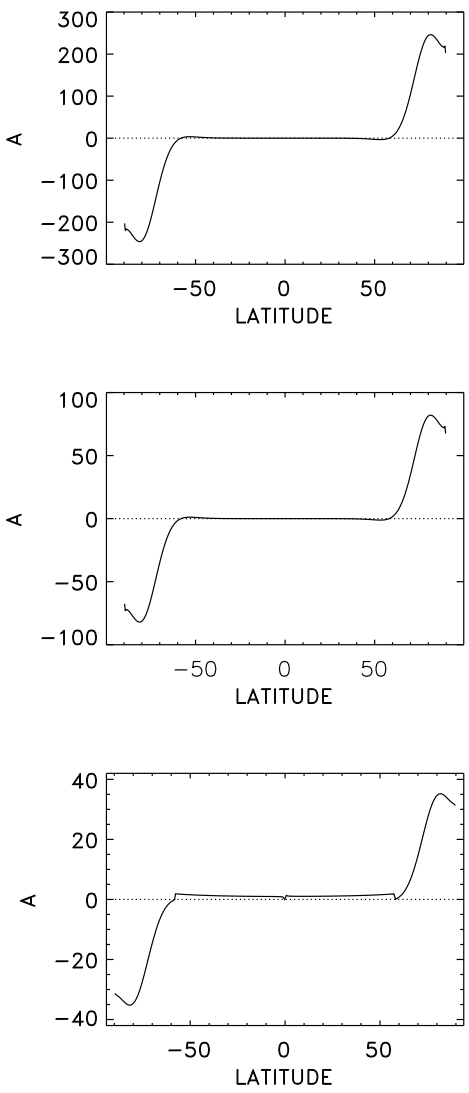

Figure 7. The normalized α effect parameter A for the modes with the highest growth rates ($m = -1$, identic for A mode and S mode). From top to bottom: $\hat{\Omega}_{\rm A,p} = 0.3$, $\hat{\Omega}_{\rm A,p} = 0.1$, $\hat{\Omega}_{\rm A,p} = 0.05$. Note i) the extreme concentration of A to the poles and ii) the A amplitudes strictly running with $\hat{\Omega}_{\rm A,p}$. For the given magnetic geometry the α effect is always positive (negative) at the northern (southern) hemisphere. $\hat{\Omega}_{\rm A} = 0.3$.

corresponding poloidal field components suppress the Tayler instability (see Rüdiger, Schultz & Elstner 2011).

For the further discussion the quantity

$$A = \frac{\mathcal{E}}{\sin\theta\cos\theta} = \frac{\alpha B_0}{u_{\rm rms} b_{\rm rms}} \frac{N}{\Omega} \tag{26}$$

is introduced which is antisymmetric with respect to the equator as expected for the (normalized) α effect. The $\sin\theta\cos\theta$ in the denominator eliminates the latitudinal profile of the toroidal field and $B_0 = \sqrt{\mu_0\rho}\, r\Omega_{\rm A}$ is its amplitude (see Eq. (2)).

Also the resulting A-profiles are highly concentrated to the poles (Fig. 7). The plots show the profiles for the weak-field cases $\hat{\Omega}_{\rm A} = 0.3$ with $\hat{\Omega}_{\rm A,p} = 0.3$, $\hat{\Omega}_{\rm A,p} = 0.1$ and $\hat{\Omega}_{\rm A,p} = 0.05$. The modes with the fastest growth produce an α effect which is always positive (negative) for positive (negative) current helicity at the northern (southern) hemisphere of the background field. The result is an α effect anticorrelated with the small-scale helicity and positively correlated with the large-scale pseudoscalar $\boldsymbol{B} \cdot {\rm curl}\boldsymbol{B}$. Exactly the same relations have been derived by nonlinear simulations of the kink-type instability for an incompressible fluid in a cylindric setup by Gellert et al. (2011). We are thus encouraged to favor the results for the modes with the highest growth rates.

For very weak poloidal field ($\hat{\Omega}_{\rm A,p} = 0.01$, not shown) the α effect is already so small (and its sign fluctuates) that the $\Omega_{\rm A,p} = 0.01$ seems to form the lower limit of the helicity production by poloidal fields.

In the weak-field regime ($\hat{\Omega}_{\rm A} < 1$) the instability excites stronger magnetic fluctuations rather than flow fluctuations. The ratio of fluctuating Alfvén velocity $v_{\rm rms} = b_{\rm rms}/\sqrt{\mu_0\rho}$ to $u_{\rm rms}$ results as $v_{\rm rms}/u_{\rm rms} \simeq 470$ for $\hat{\Omega}_{\rm A} = 0.01$ and $v_{\rm rms}/u_{\rm rms} \simeq 46$ for $\hat{\Omega}_{\rm A} = 0.1$. Hence, we find

$$\frac{v_{\rm rms}}{u_{\rm rms}} \simeq \frac{4.7}{\hat{\Omega}_{\rm A}} \tag{27}$$

for weak fields. For strong fields ($\hat{\Omega}_{\rm A} > 1$) the fluctuations become close to equipartition, i.e. $v_{\rm rms} \simeq u_{\rm rms}$.

5 DYNAMO THEORY

On the basis of the obtained informations about the α effect (amplitude and latitudinal profile) we have to probe the possible existence of a dynamo mechanism.

5.1 Eddy diffusivity

We start to estimate the typical velocity perturbation and the eddy magnetic-diffusivity. We write $u \simeq \lambda/\tau$ and use the growth time $\tau_{\rm gr} = 1/\gamma$ as the timescale τ. Hence,

$$u \simeq \gamma\lambda = \pi\hat{\gamma}\hat{\lambda}\frac{\Omega^2 r}{N}. \tag{28}$$

The first step holds for purely toroidal fields ($\Omega_{\rm A,p} = 0$). From Fig. 3 (top) one finds $\hat{\gamma}\hat{\lambda} \equiv 10^{-4}$ so that with solar values $u \simeq 1$ mm/s results. The estimate $\eta_{\rm T} \simeq u\lambda$ leads to $\eta_{\rm T} \simeq 10^5$ cm^2/s as the order of magnitude of the eddy diffusivity. The value increases for fast rotating giants by one or two orders of magnitudes. It perfectly fits the diffusion coefficients for chemicals which are needed to explain the weak lithium depletion of solar type stars (Barnes, Charbonneau & MacGregor 1999).

The same estimate $\eta_{\rm T} \simeq \gamma\lambda^2$ yields

$$\eta_{\rm T} \simeq \pi^2\hat{\gamma}\hat{\lambda}^2\frac{\Omega^2}{N^2}\Omega r^2. \tag{29}$$

The three examples for helical background fields given in Fig. 5 lead to a common value of $\hat{\gamma}\hat{\lambda}^2 \simeq 10^{-6}$. Hence, $\eta_{\rm T} \simeq 3\cdot 10^5$ cm^2/s results for the upper radiation zone of the Sun. This value is very close to the above estimation for purely toroidal fields. It is increased by more than three orders of magnitudes if more massive stars are considered. Figure 1 shows the details of a model with a mass of $3M_\odot$ and 10 days rotation period.

5.2 Dynamo conditions

The α effect enters the dynamo theory via the dimensionless dynamo number

$$C_\alpha = \frac{\alpha\ r}{\eta_{\rm T}}. \qquad (30)$$

Equation (26) together with the heuristic relation $u^2/\eta_{\rm T} \simeq \gamma$ directly provides

$$C_\alpha\ =\ \frac{5}{\hat\Omega_{\rm A}^2}\frac{\Omega}{N}\ \hat\gamma\ A. \qquad (31)$$

Hence, the product $\hat\gamma A$ determines the effectivity of the α effect. With $\hat\gamma\ A \simeq 0.03$ a value of $C_\alpha \simeq 10^{-(2...3)}$ results for the solar model. Note that the buoyancy frequency linearly enters the equation. Also for the $3M_\odot$ star of Fig. 1 the $C_\alpha\ \simeq\ 0.1$ remains small. The operation of a (stationary) α^2 dynamo is thus excluded for radiation stellar zones. The existence of an (oscillating) $\alpha\Omega$ dynamo, however, remains possible. All $\alpha\Omega$ dynamos can work with very small α effect if only C_Ω

$$C_\Omega = \frac{\Omega_0\ r^2}{\eta_{\rm T}}. \qquad (32)$$

is high enough and this is always possible for sufficiently small eddy diffusivity $\eta_{\rm T}$. The only consequences of very small α effect are i) that the ratio of toroidal and poloidal magnetic field components becomes very large and ii) also the growth time of the dynamo instability becomes large. The growth time of the weakly supercritical $\alpha\Omega$ dynamo for $\eta_{\rm T} \simeq 10^5{\rm cm}^2/{\rm s}$ is extremely long (order of Gyrs for the Sun). With (say) 3% differential rotation this value of the eddy diffusivity leads for the Sun to C_Ω of order 10^7.

There is another possibility to proceed. For all $\alpha\Omega$ dynamos the ratio β of the toroidal and the radial field amplitudes is

$$\beta \simeq \epsilon\sqrt{\frac{C_\Omega}{C_\alpha}}. \qquad (33)$$

The scaling parameter ϵ is about 0.05 (see Table 1). Hence, $C_\Omega \simeq \beta^2 C_\alpha/\epsilon^2$. The excitation condition for such dynamos can be written as

$$C_\alpha C_\Omega = D_{\rm crit}, \qquad (34)$$

where $D_{\rm crit}$ runs inversely with the shear. With (33) $C_\alpha \gtrsim \sqrt{\epsilon^2 D_{\rm crit}}/\beta$ results as excitation condition. One finds

$$\hat\gamma A \gtrsim \frac{\epsilon}{5}\sqrt{D_{\rm crit}}\hat\Omega_{\rm A,p}\hat\Omega_{\rm A} \qquad (35)$$

for fixed shear. Note that the condition (35) does no longer contain the stellar parameters like Ω/N and/or the radius. The following findings are thus valid for all stellar radiation zones.

Our first example is formed by $\hat\Omega_{\rm A} = 0.3$ and $\hat\Omega_{\rm A,p} = 0.3$. The condition (35) then reads $\hat\gamma A \gtrsim 0.06\epsilon\sqrt{D_{\rm crit}}$. As we shall see below, a typical value for the dynamo number is $\epsilon\sqrt{D_{\rm crit}} \simeq 30$ so that for dynamo excitation

$$\hat\gamma A \gtrsim 2\hat\Omega_{\rm A,p}. \qquad (36)$$

This relation must be read as an equation for the supercritical value of $\hat\Omega_{\rm A,p}$. The excitation is thus formally more easy for smaller poloidal field. After the numerical results in the Figs. 5 (top) and 7 (top) one finds $\hat\gamma A \simeq 10^{-3}$ for $\hat\Omega_{\rm A,p} = 0.3$ which is by far too small. For $\hat\Omega_{\rm A,p} = 0.1$ it is $\hat\gamma A \simeq 0.03$ which is also not supercritical. The comparison of the Figs. 5 and 7 demonstrates that for large poloidal fields the A grows but in the same time the growth rate drastically sinks which indicates the stabilizing action of the poloidal fields. An $\alpha\Omega$ dynamo in radiation zones cannot work, therefore, with too strong poloidal fields.

Note that with $\hat\gamma A \simeq 0.2$ for $\hat\Omega_{\rm A,p} = 0.05$ the condition (36) can be fulfilled due to the increase of the growth rate. For smaller $\hat\Omega_{\rm A,p}$ the ability of the poloidal field to create a coherent α effect sinks. For $\hat\Omega_{\rm A,p} = 0.01$ the function A has already two signs at either hemisphere. However, as the condition (36) can be fulfilled the existence of an $\alpha\Omega$ dynamo cannot be excluded by the numerical results. We must thus solve the dynamo equations in order to probe the existence of such dynamos which work with very small values of the α effect.

The α effect plotted in Fig. 7 shows another complicating characteristics, i.e. its concentration at the poles. In the next Section nonlinear $\alpha\Omega$ dynamo models are thus constructed with a weak solar-type latitudinal differential rotation and an α effect which is concentrated at the poles. It is known from the theory of $\alpha\Omega$ dynamos operating with $\cos\theta$ profiles of the α effect that they produce too polar butterfly diagrams. We must thus expect that the existence of $\alpha\Omega$ dynamos to produce mid-latitude belts like in Eq. (2) with pole-concentrated α effect is unlikely.

5.3 Dynamo models

The influence of the polar concentration of magnetic-induced α effect on a possible $\alpha\Omega$ dynamo can easily be probed. The stability of an axisymmetric toroidal background field has been considered so that only the numerical values of an axisymmetric α are known. This scenario is only consistent if the possible $\alpha\Omega$ dynamo produces axisymmetric toroidal field belts at the latitude of the original background field. We know that this is true for an α effect (plus solar-type differential rotation) with the standard $\cos\theta$-profile. We have to check, therefore, whether this result remains true for the α effect concentrated close to the poles.

To this end a simple model is constructed. In a spherical shell between the normalized radii 0.6 and 1 the rotation frequency is $\Omega = C_\Omega(1 - 0.03\cos^2\theta)$. The small value of the relative shear allows to consider the fluid as hydrodynamically stable (see Watson 1981). Possible production of hydrodynamic-induced α effect in radiative zones such as that by Dikpati & Gilman (2001) is therefore excluded. The shear peaks at 45° which is the same latitude as that of the peak of the toroidal field. To model the polar concentration of the magnetic-induced α effect the expression

$$\alpha = C_\alpha\ \cos^\ell\theta \qquad (37)$$

is used with the free parameter ℓ fixing the latitudinal profile of the α effect. The polar concentration presented in Fig. 7 leads to rather high values of ℓ. A perfect-conductor boundary condition is used at the inner radius. The outer computing domain is extended to the radius 1.2. Outside the stellar surface the diffusivity is increased by a factor of 10. For the outermost boundary a pseudovacuum condition is used. The method of a global quenching of the α effect is

used in order to find the characteristic eigenvalue of marginal dynamo instability (Elstner, Meinel & Rüdiger 1989).

Table 1 presents the numerical results for a reference dynamo model with 3% differential rotation and for $C_\Omega = 257,000$. Only the numbers are given for marginal dynamo instability. If the real C_α differs from the reference C_α by a factor $1/\gamma$ then the resulting β also differs by the factor γ, so that

$$\beta C_\alpha = \beta^{\rm ref} C_\alpha^{\rm ref} \simeq 30. \qquad (38)$$

This condition is automatically fulfilled for all dynamo models which fulfill the excitation condition (35) independent on the particular stellar model. All the dynamos listed in Table 1 provide positive (negative) values of the large-scale current helicity $\boldsymbol{B} \cdot \mathrm{curl}\boldsymbol{B}$ at the northern (southern) hemisphere. As we have assumed the same constellation for the above background field producing the α effect the theory is thus consistent under this aspect.

We have also to probe whether the star rotates fast enough to produce sufficiently large C_Ω for the required dynamo numbers of the reference values of Table 1. It is

$$C_\Omega = \frac{D_{\rm crit}}{C_\alpha} = \frac{\sqrt{D_{\rm crit}}}{\epsilon} \frac{\hat\Omega_{\rm A}}{\hat\Omega_{\rm A,p}} \frac{N}{\Omega}. \qquad (39)$$

Note at first that the excitation is much more easy for massive stars as their N/Ω is smaller (Fig. 1). Inserting the characteristic numbers of our models the result is $C_\Omega \gtrsim 10^5\ N/\Omega$ which is fulfilled by both the considered stellar models by their estimated values $C_\Omega \simeq 10^{10}$. Either the Sun as the considered hot stars with rotation periods of a couple of days rotate fast enough the excite an $\alpha\Omega$ dynamo with a very weak shear (3%).

To discuss the influence of the quantity ℓ we present models with $\ell = 1$, $\ell = 5$ and $\ell = 15$. The latter value describes the strongest concentration of the α effect to the poles. For $\ell = 1$ (i.e. $\alpha \propto \cos\theta$) the dynamo-generated toroidal field peaks exactly at $\theta = 45°$ so that the presented stability analysis which bases on a toroidal field which also peaks at $\theta = 45°$ (see Eq. (2)) would be consistent. This case together with the excitation condition (36) which is fulfilled by the magnetic amplitudes $\hat\Omega_{\rm A} = 0.3$ and $\hat\Omega_{\rm A,p} = 0.05$ would strongly suggest the existence of an $\alpha\Omega$ dynamo in magnetized radiation zones of hot stars.

However, the models listed in Table 1 provide the result that the induced toroidal field belts become more and more concentrated to the poles for increasing ℓ. This behavior is insofar not trivial as the generation of the toroidal field by the differential rotation does *not* depend on ℓ. Such polar belts resulting for $\ell > 1$ can never reproduce the mid-latitudinal belts of Eq. (2) on which the α effect bases. The first example of Fig. 8 (top) is the standard $\alpha\Omega$ dynamo with the latitudinal profile $\alpha \propto \cos\theta$. It produces axisymmetric toroidal magnetic belts of dipolar symmetry at the same latitude where the shear $\partial\Omega/\partial\theta$ has a maximum. For growing ℓ the belt position drifts more and more polewards (the field position becomes $45° > \theta > 135°$). It is thus *not possible* to maintain toroidal field belts in mid-latitudes if the α effect mainly exists in the polar region ($\ell > 1$).

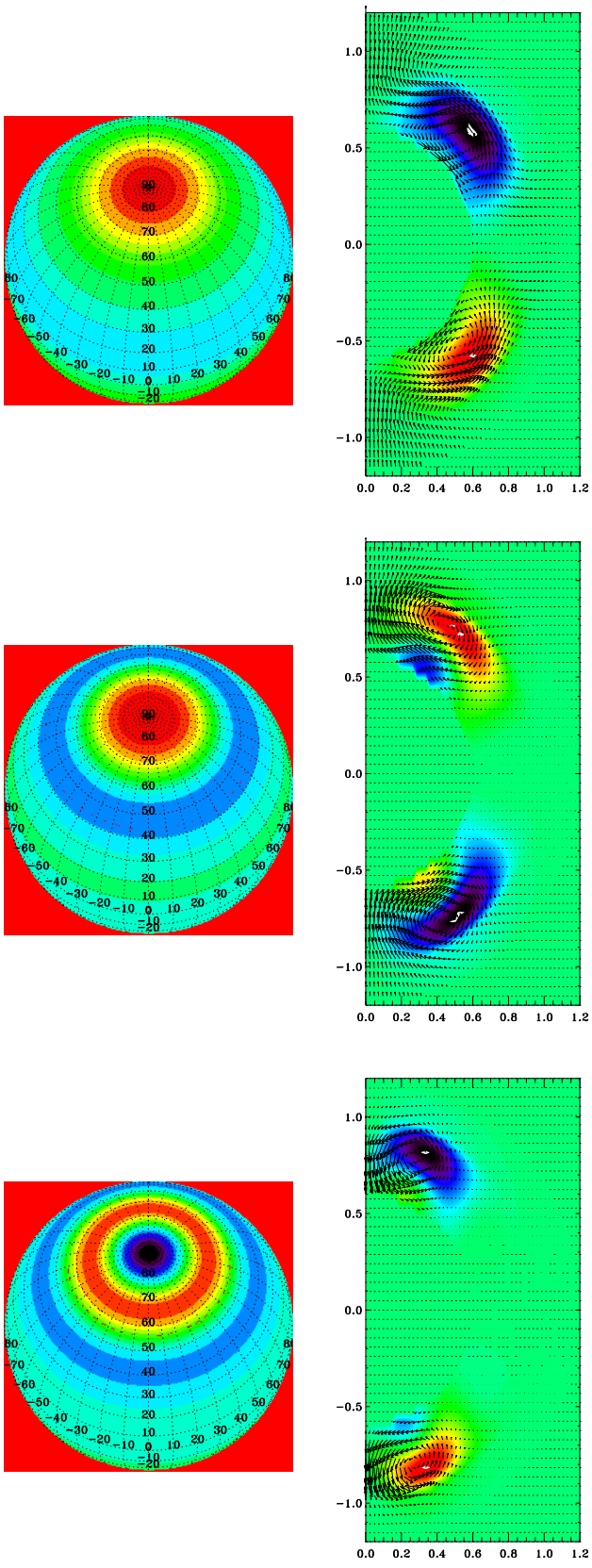

Figure 8. The field geometry of $\alpha\Omega$ dynamo models with $\ell = 1$ (top), $\ell = 5$ (middle), $\ell = 15$ (bottom). Left: radial field at the surface. Right: toroidal field pattern. The magnetic field belts are drifting radially during the cycle.

Table 1. Reference dynamo models with 3% differential rotation and for $C_\Omega = 257,000$. The last column gives the polar distance of the maximum position of the northern toroidal field belt.

ℓ	$D_{\rm crit}$	C_α	β	ϵ	$\epsilon\sqrt{D_{\rm crit}}$	θ
1	118,000	0.46	56	0.07	26	45°
5	347,000	1.35	23	0.05	31	38°
15	976,000	3.8	6.3	0.02	24	23°

6 CONCLUSIONS

It is demonstrated with a linear theory that the Tayler instability of a toroidal magnetic field in a density-stratified radiation zone of hot stars does not produce helicity and/or α effect. If, however, a weak poloidal field component is added forming a large-scale current helicity $\boldsymbol{B}\cdot{\rm curl}\boldsymbol{B}$ then the instability leads to small-scale helicity, current helicity and also to α effect. If $\boldsymbol{B}\cdot{\rm curl}\boldsymbol{B}$ is *positive* in the northern hemisphere then the helicity $\langle\boldsymbol{u}\cdot{\rm curl}\boldsymbol{u}\rangle$ is *negative* at the northern hemisphere if only the modes are considered which grow fastest. Hence, the small-scale kinetic helicity and the large-scale current helicity of the background field are anticorrelated.

As it is often the case, the corresponding α effect is anticorrelated with the kinetic helicity and, therefore, positively correlated with the large-scale current helicity $\boldsymbol{B}\cdot{\rm curl}\boldsymbol{B}$. The calculations lead to two basic properties of this α effect. It is i) small, i.e. the normalized value C_α is only of order $10^{-(2...3)}$ and ii) concentrated at the poles. The first property excludes the existence of α^2 dynamos in radiative zones and the second property makes the existence of $\alpha\Omega$ dynamos (with weak differential rotation in mid-latitudes) unlikely. As we have shown only a dynamo with $\alpha\propto\cos\theta$ produces the toroidal fields in mid-latitudes. For $\ell>1$, however, the belts are more and more shifted into the polar region. Such fields cannot close the loop of field amplification by reproducing the original axisymmetric toroidal field.

Or, with other words, the rotation law with the considered profile ($\Omega\propto\cos^2\theta$) mainly induces toroidal fields at mid-latitudes where for high values of ℓ almost no α effect exists. Hence, an $\alpha\Omega$ dynamo could only work for very fast rotation. By very fast rotation the instability is suppressed (see Fig. 2). This topological problem seems to be the key problem with the magnetic-driven dynamo rather than the excitation conditions for $\alpha\Omega$ dynamos. It is, however, not yet clear whether this argumentation also holds with the same power with other than the used rotation laws and/or in fully nonlinear simulations. All the presented $\alpha\Omega$ dynamo models working with a weak solar-type differential rotation are reproducing the assumed sign of the large-scale current helicity $\boldsymbol{B}\cdot{\rm curl}\boldsymbol{B}$. If thus the dynamo produces its own α effect by the magnetic instability then the signs will be consistent.

A basic deficit of the presented theory is the fact that both helicity and α effect have been computed in rigidly rotating stars while for an $\alpha\Omega$ dynamo the rotation must be nonrigid. It might be the case that growth rates and magnetic patterns of the Tayler instability are strongly modified by even weak differential rotation. The discussion of this new subject, however, is not the scope of the present paper. We have thus considered only cases with a rather weak differential rotation (3 %).

Another deficit is formed by the order-of-magnitude estimation of the eddy diffusivity. Using the characteristic scales of the modes with the highest growth rates the typical velocity is of order 1 mm/s and the typical diffusivity value is about 10^5 cm^2/s (both for solar values). Estimations of the radial mixing produced by the same instability provide an important test of the theory. The observed content of light elements at the Sun impose restrictions on radial mixing in the upper radiative core (Barnes et al. 1999, and references therein). The chemical mixing in the deep stellar interior can also be compatible with observations only if its characteristic time is longer than the evolutionary time scale (Kippenhahn & Weigert 1994). Only very slightly supercritical kink-type instability can satisfy this restriction (Kitchatinov & Rüdiger 2008).

All the material values in the paper are solar values. The formulation of the dynamo theory is such that the material parameters of the stellar interior do not appear (see Eq. (35)). The conclusions about the dynamo activity for hot stars do thus not depend on the mass of the star. This is not true, however, for the above mentioned order-of-magnitude estimations of the characteristic values of velocity and diffusivity which are running with Ω/N and $(\Omega/N)^2$, resp. From Fig. 1 one finds that the given solar values increase by factors of 30 or 900, resp., for stars with three solar masses.

Only nonlinear simulations can demonstrate whether the system indeed prefers the modes with the highest growth rates. Only if not then the radiative-zone dynamo has a chance to work in the solar interior but if it works then it should be only marginally supercritical.

ACKNOWLEDGMENTS

LLK is grateful to the Deutsche Forschungsgemeinschaft for the support of the project (436 RUS 113/839).

REFERENCES

Barnes G., Charbonneau P., MacGregor K.B., 1999, ApJ, 511, 466
Brandenburg A., Nordlund Å., Stein R.F., Torkelsson U., 1995, ApJ, 446, 746
Cally P.S., 2003, MNRAS, 339, 957
Chandrasekhar S., 1961, Hydrodynamic and Hydromagnetic Stability. Clarendon Press, Oxford
Chatterjee, P., Mitra, D., Brandenburg A., Rheinhardt, M., 2010, PRE, (in press)
Cowling T.G., 1933, MNRAS, 94, 39
Dikpati M., Gilman, P.A., 2001, ApJ, 559, 428
Dudley M.L., James, R.W., 1989, Proc. Royal Soc. London A, 425, 407
Elsasser W.M., 1946, Phys. Rev., 69, 106
Elstner D., Meinel R., Rüdiger G., 1989, Geophys. Astrophys. Fluid Dyn., 50, 85
Fromang S., Papaloizou J., 2007, A&A, 476, 1113
Fromang S., Papaloizou J., Lesur G., Heinemann T., 2007, A&A, 476, 1123

Gellert M., Rüdiger G., Hollerbach R., 2011, MNRAS, 414, 2696
Goossens M., Biront D., Tayler R.J., 1981, Ap&SS, 75, 521
Hawley J.F., Gammie C.F., Balbus S.A., 1996, ApJ, 464, 690.
Kippenhahn R., Weigert A., 1994, Stellar Structure and Evolution. Springer, Berlin
Kitchatinov L.L., Rüdiger G., 2008, A&A, 478, 1 (KR08)
Kitchatinov L.L., Rüdiger G., 2009, A&A, 504, 303
Paxton B., 2004, PASP, 116, 699
Pitts E., Tayler R.J., 1985, MNRAS, 216, 139
Rüdiger G., Kitchatinov L.L., 2010, Geophys. Astrophys. Fluid Dyn., 104, 273
Rüdiger G., Gellert M., Schultz M., Hollerbach R., 2010, Phys. Rev. E, 82, 016319
Rüdiger G., Schultz M., Elstner D., 2011, A&A, 530, 55
Spruit H.C., 1999, A&A, 349, 189
Spruit H.C., 2002, A&A, 381, 923
Tayler R.J., 1973, MNRAS, 161, 365
Tout C.A., Pringle J.E., 1992, MNRAS, 259, 604
Watson M., 1981, Geophys. Astrophys. Fluid Dyn., 16, 285

This paper has been typeset from a TEX/ LATEX file prepared by the author.